Local suppression of Josephson currents in niobium/two-dimensional electron gas/niobium structures by an injection current

K. Neurohr, Th. Schäpers, J. Malindretos, S. Lachenmann, A. I. Braginski, and H. Lüth
Institut für Schicht- und Ionentechnik, Forschungszentrum Jülich, D-52425 Jülich, Germany

M. Behet and G. Borghs
Interuniversity Microelectronics Center, Kapeldreef 75, B-3001 Leuven, Belgium

A. A. Golubov
Faculty of Applied Physics, University of Twente, P.O. Box 217, 7500 AE Enschede, The Netherlands
(Received 9 December 1998)

We investigated niobium-AlGaSb/InAs-niobium hybrid structures using a high mobility two-dimensional electron gas as a weak link. The Josephson current observed in this structure was suppressed by an injection current driven into the weak link via an additional normal lead. Using a four-terminal configuration the supercurrent is suppressed all over the weak link. In a three-terminal configuration it was possible to suppress the supercurrent locally. [S0163-1829(99)06217-7]

The semiconductor/superconductor hybrid structure has been the subject of extensive research during the last years, to prove its suitableness as an interface between superconductor and semiconductor electronics. Especially the control of the supercurrent in a weak-link structure has attracted considerable interest in recent years.[1] One approach was to transfer the well-known semiconductor field effect transistor to superconductor/two-dimensional electron gas (2DEG) structures as proposed by Clark *et al.*[2] The supercurrrent flowing through the 2DEG was switched off by reducing the coherence length in the channel by applying a negative gate voltage.[3,4] Since the voltage necessary for depleting the electrons in the 2DEG channel is typically of the order of the band gap of the semiconductor and the output signal of the order of the superconducting gap of the electrodes, a voltage gain is hard to achieve. An alternative concept to avoid this problem is controlling the supercurrent by the injection of electrons via an additional nonsuperconductive contact into the weak link.[5–8] The energy of these carriers should be only of the order of the superconducting gap of the electrodes. Very recently, the control of the supercurrent by an injection current was experimentally succeeded for a Nb/Au weak link structure.[9] This system was in the diffusive regime with inelastic scattering processes thermalizing the injected carriers.

In our current-controlled structure the superconductor Nb was contacted to a high-mobility two-dimensional electron gas (2DEG) in an $Al_{0.2}Ga_{0.8}Sb$/InAs heterostructure. Due to the high electron mobility the carrier transport from one Nb electrode to the opposite one can be considered to be ballistic. In addition inelastic scattering should become relevant only for higher temperatures. For weak links without inelastic scattering an even more efficient tuning of the Josephson current was predicted compared with the case of inelastic scattering present.[10] It will be shown that if a current is injected via Ohmic contacts into the 2DEG in a four-terminal configuration the supercurrent can be suppressed completely. In a three-terminal configuration it was possible to suppress the supercurrent locally, which was proven by measuring and fitting the interference patterns of the Josephson current appearing when a magnetic field is applied to the weak link.

The heterostructure which forms the weak link in our structure was grown by molecular-beam epitaxy on a semi-insulating GaAs substrate. After a 1100 nm Al-Ga-Sb buffer layer, a 500 nm GaSb grading was grown followed by 50 nm $Al_{0.2}Ga_{0.8}Sb$ as a barrier and the 15 nm InAs channel. The layer structure was finally capped by a 20 nm $Al_{0.2}Ga_{0.8}Sb$ barrier.[11]

In order to fabricate samples with a distance between the niobium electrodes shorter than the superconducting coherence length ξ_0^N in the 2DEG we used a self-aligning process with a negative resist (AZ PN 114) for electron-beam lithography.[12] In order to be able to contact the 2DEG via the normal leads first a patterned Pd/Au (15nm/150nm) layer was alloyed to the 2DEG for 60 s at 260°C. Then the semiconductor structure including the weak link and the leads for the normal injection current was defined in the resist. After a prebake of the resist at 120°C for 120 s this structure was written with a 50 keV electron beam. The post exposure bake was performed at 105°C for 5 min. The pattern was now transferred to the 2DEG by using the resist as an etching mask for 300 eV Argon ions in a HV chamber ($p=1\times10^{-6}$ mbar). After this, the niobium was deposited by sputtering ($T_c\sim6.5$ K) in the same chamber without breaking the vacuum. To separate the niobium electrodes the AZ PN 114 resist was used for a lift-off step performed by n-Methyl-2-Pyrollidon at 190°C.

The electrical transport data of the 2DEG were obtained from quantum Hall and Shubnikov–de Haas measurements yielding an electron sheet concentration of 8.3×10^{11} cm^{-2} and a high electron mobility of 300 000 cm^2/Vs at a temperature of 0.6 K. Temperature-dependent Shubnikov–de Haas measurements showed an effective electron mass of $0.037\,m_e$. These values result in an elastic mean free path l_{el} of $4.45\,\mu$m.

The complete structure is shown schematically in Fig. 1. The contact length W was 6.6 μm, the spacing d of the

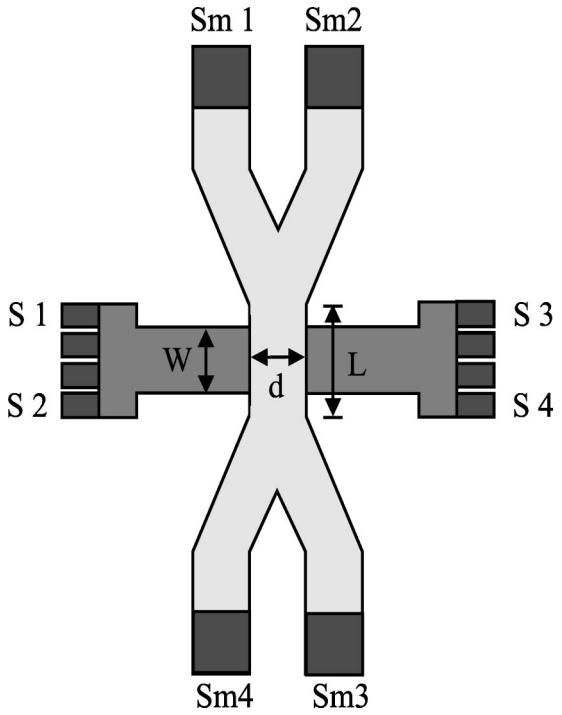

FIG. 1. Schematic of the sample layout. Sm 1–4 denotes semiconductor contacts, S 1–4 are contacts to the niobium electrodes. $W=6.6\ \mu$m; $L=7\ \mu$m; $d=280$ nm.

electrodes 280 nm. The leads labeled with Sm 1–4 are Ohmic contacts alloyed to the 2DEG for injecting electrons via the control line into the weak link; those labeled S 1–4 are contacted on the niobium electrodes to impose the Josephson current and measure the voltage drop across the weak link.

Figure 2 shows the I-V curves of our Josephson junction at $T=0.6$ K for different currents injected from Sm 1 to Sm 3 (see Fig. 1). The Josephson current was driven from S 1 to S 3 and the voltage measured between S 2 and S 4. Without injection current the sample exhibits a critical current of 952 nA and an $I_C R_N$ product of about 65 μV. By raising the injection current the critical current gradually decreases, until for $I_{\rm inj}=2.5\mu$A I_C vanishes.

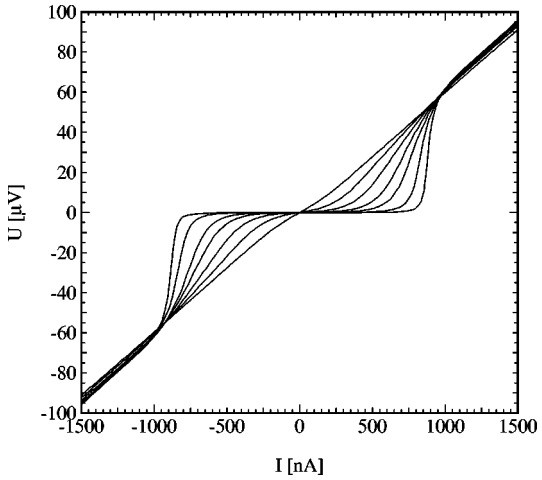

FIG. 2. *I-V* characteristics of the Josephson contact at $T=0.6$ K. The injection currents suppressing the supercurrent are: 0; 100; 200; 350; 600 nA; 2.5 μA.

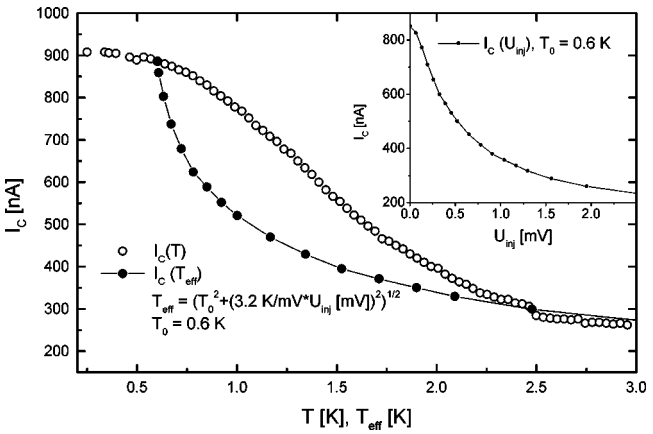

FIG. 3. Critical current of the junction plotted vs temperature (open circles) and vs. an effective temperature calculated from the energy of the injected carriers (solid circles). Inset: Dependence of the critical current on the voltage drop along the control line.

The mechanism responsible for the supercurrent suppression is a nonequillibrium population of the Andreev levels which are generated by multiple phase-coherent Andreev reflection of electrons and holes at the two interfaces of the 2DEG to the Nb electrodes.[7] In our structure the separation of the Nb banks d is smaller than the elastic mean free path l_e, therefore, the transport can be described within the ballistic regime. In this limit, the Josephson current is carried by discrete Andreev levels within the superconductive gap Δ as well as by continuum levels outside Δ.[13] Only two bound Andreev levels at $E(\phi=0)=\pm\Delta$ will be present in the 2DEG, if d is also smaller than the coherence length $\xi_0^N=\hbar v_{FN}/(2\Delta)$. Here ϕ is the phase difference of the two superconducting electrodes and v_{FN} is the Fermi velocity in the 2DEG. At zero temperature only the lower one of these levels is occupied, carrying electrons moving in the direction of the externally driven current and holes moving in the opposite one. Populating the upper level with electrons, e.g., by raising the temperature of the system leads to an additional current flowing in the opposite direction. The supercurrent flowing in the weak link is the net current resulting from the currents carried by the two Andreev levels. This is still an equilibrium situation since the whole sample is at the same temperature. A nonequilibrium population of these levels can be created, e.g., by injecting electrons, done as described above in our 2DEG populating the upper Andreev level. Since the temperature of the carriers is higher than the lattice temperature and phonon scattering can be neglected the suppression of the Josephson current is a nonequilibrium effect. In our sample $\xi_0^N\sim 200$ nm $<d=280$ nm holds, so more than two levels will evolve but the physical mechanism of the suppression of the supercurrent is the same.[7]

The inset in Fig. 3 shows the dependence of the critical current on the the voltage drop U_{inj} along the control line, which was measured between Sm 2 and Sm 4 (see Fig. 1) at $T_0=0.6$ K. Since I_C was determined by a criterion of 10 μV, the saturation value is not zero but 200 nA. The voltage drop can be associated with the energy of the injected carriers if inelastic scattering in the control line can be neglected. The inelastic scattering length $l_{\rm inel}$ can be calculated by the formula of Giuliani and Quinn[14] for excess energies small com-

pared to the Fermi energy. For our sample $E_F = 30$ meV results in $l_{\text{inel}} \sim 7\,\mu$m for an excess energy of 2 meV. This length is in the range of the extension of the control line. For smaller energies l_{inel} becomes larger and the carriers will keep their initial distribution function. This function along the control line is a double-step structure caused by the superposition of the energy distributions in the two normal reservoirs contacted to the weak link. Pothier *et al.* recently measured this double-step distribution function in a diffusive metal wire.[15] Another strong hint for nonthermal carriers injected in the weak link shows the comparison of the temperature dependence of the critical current with an effective temperature presentation of the $I_C(U_{\text{inj}})$ data in Fig. 3. The plateau in the $I_C(T)$ dependence results from the nonzero probability for normal reflection at the two Nb-2DEG interfaces. This opens up a gap in the $E_n(\phi)$ relation which has to be overcome by the thermally excited carriers.[7] The plateau should be observable also in the $I_C(U_{\text{inj}})$ presentation if measured at temperatures lower than 0.6 K which is indicated by the turning point of the curve in the inset for small voltages. The calculation of the effective temperature from the formula $T_{\text{eff}}(x) = \sqrt{T_0^2 + x/L(1-x/L)(3e^2/\pi^2 k_B^2)U_{\text{inj}}^2}$ was done for the middle of the control line ($x = L/2$).[15] The number of the injected carriers at this position is reduced since a part flows through the niobium electrodes, which act as a parallel path. Following the calculations of Kupriyanov in Ref. 16 we estimate the length over which the $1/e$th part of the injected carriers flows into the electrodes to about 1 μm. Thus, for reasons of symmetry the supercurrent is suppressed most effectively at both edges of the Josephson contact. As will be shown below the amount of supercurrent flowing through the middle of the weak link is smaller than at the edges anyway. Both curves in the temperature presentation in Fig. 3 should therefore not coincide exactly, but the deviation should not be qualitatively if the injected carriers are completely thermalized by inelastic scattering. This is but the case up to excess energies of about 2 meV when l_{inel} equals the length of the control line. Therefore our sample is in a different regime than those of Morpurgo *et al.*,[9] who successfully applied the effective temperature model to their samples. It was shown that for diffusive weak links without inelastic scattering an even more efficient tuning of the Josephson current should be possible compared with the case of inelastic scattering present.[10] Our sample is not in the diffusive regime since the elastic mean free path is of the order of several μm but the roughness of the 2DEG/Nb interface caused by the argon ion etching ensures a nearly isotropic momentum distribution of the injected electrons in the wire. An effective suppression of the supercurrent would be not possible if the electron momentum is directed only along the control line since the carrier wave function could not couple to the Andreev levels generated by electrons and holes moving perpendicular to the control line.

Besides the energy dependence of the distribution function in the weak link, the distribution of the Josephson current is of interest. By applying a magnetic field to the contact oriented perpendicular to the plane of Fig. 1 the phase difference along the contact is controllable and yields information about the profile of the supercurrent in the 2DEG. Figure 4 shows the dependence of the critical current on the magnetic flux through our contact, normalized to the magnetic

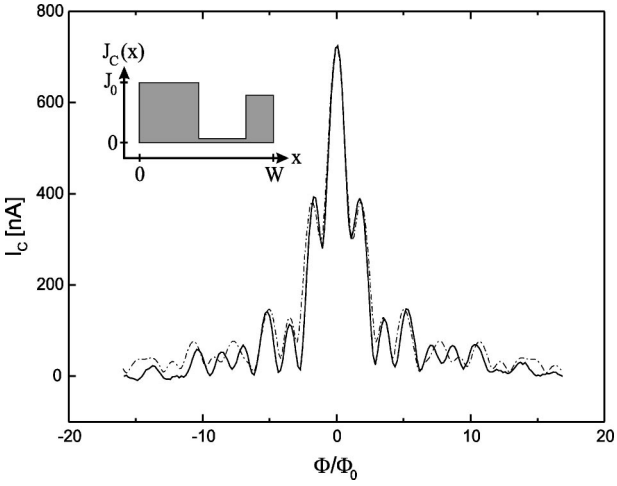

FIG. 4. Fraunhofer pattern of the contact without injection current (solid line). The fit using the current distribution shown in the inset is dash-dotted.

flux quantum, without any injection current applied (solid line). The effective magnetic field present at the contact due to focusing of the applied field B_0 by Meissner screening currents in the electrodes was calculated by $B_{\text{eff}} = (2W/d)^{2/3} \times B_0$.[17] The best fit was obtained by assuming a contact area of 70% of the area defined by lithography. This fit is shown by the dash-dotted curve in Fig. 4. The distribution of the Josephson current assumed here is shown in the inset. The higher current densities at the edges of the contact can be explained by the fact that our sample is in the intermediate regime between a long and a short junction ($W \simeq \lambda_J, \lambda_J$ is the Josephson penetration depth). The asymmetry is most probable due to contact inhomogeneity.

By injecting carriers in a three terminal configuration, using one niobium electrode as a common ground for both current sources, the supercurrent is effected not in the whole weak link but is more strongly suppressed in the part where the injection takes place. Measuring the Fraunhofer pattern

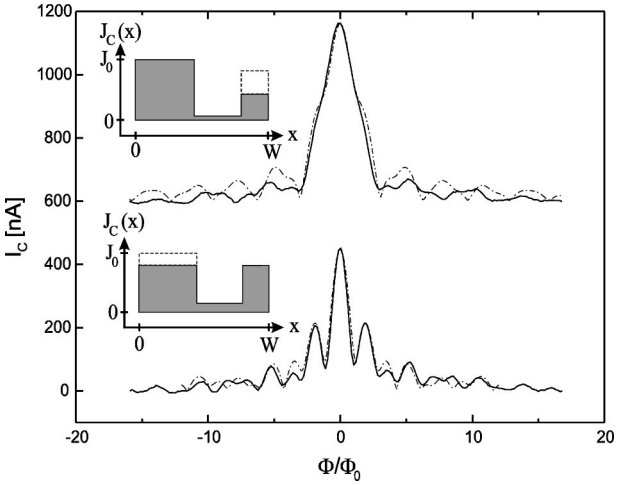

FIG. 5. Fraunhofer pattern of the contact with current of 500 nA injected via Sm 1–S 3 (lower pattern, solid line) and with a current of 700 nA injected via Sm 4–S 4 (solid line, pattern shifted by 600 nA). The fits using the current distributions shown in the insets are the dash-dotted lines.

in this configuration shows this effect indeed (Fig. 5). The lower pattern (solid line) results from injecting the carriers from Sm1 to S 3 (see Fig. 1), reducing the Josephson current stronger on the side of the weak link where the larger amount of the supercurrent flows without injection current (see inset Fig. 4). The pattern now shows a superconducting quantum interference device-like form with all minima nearly going to zero. The best fit (dash-dotted line) is achieved now by assuming a more symmetric current profile (lower inset Fig. 5). The effect of injecting via Sm 4 to S 4 leads to a very asymmetric distribution of the supercurrent in the weak link leading to a pattern as shown by the shifted, solid curve in the upper part of Fig. 5. The discrepancy between measurements and fits for higher fields is caused by deviations of the real current distribution from the assumed steplike one.

In summary, we demonstrated the complete suppression of a Josephson current flowing in a 2DEG by injecting electrons to the weak link via an additional normal lead. The local effect of this tuning was shown by magnetic-field-dependent measurements.

The authors thank A. van der Hart and G. Crecelius for their contribution to the results summarized here. The excellent assistance of G. Müllejans during the measurements is greatly appreciated.

[1] A. W. Kleinsasser and W. J. Gallagher, in *Superconducting Devices*, edited by S. T. Ruggiero and D. A. Rudman (Academic, San Diego, 1990).
[2] T. D. Clark, R. J. Prance, and A. D. C. Grassie, J. Appl. Phys. **51**, 2736 (1980).
[3] H. Takayanagi, T. Akazaki, J. Nitta, and T. Enoki, Jpn. J. Appl. Phys., part 1 **34**, 1391 (1995).
[4] T. Akazaki, H. Takayanagi, J. Nitta, and T. Enoki, Appl. Phys. Lett. **68**, 418 (1996).
[5] B. J. van Wees, K.-M. H. Lenssen, and C. J. P. M. Harmans, Phys. Rev. B **44**, 470 (1991).
[6] A. F. Volkov, Phys. Rev. Lett. **74**, 4730 (1995).
[7] Li-Fu Chang and P. F. Bagwell, Phys. Rev. B **55**, 12 678 (1997).
[8] P. Samuelsson, V. S. Shumeiko, and G. Wendin, Phys. Rev. B **56**, R5763 (1997).
[9] A. F. Morpurgo, T. M. Klapwijk, and B. J. van Wees, Appl. Phys. Lett. **72**, 966 (1997).
[10] F. K. Wilhelm, G. Schön, and A. D. Zaikin, Phys. Rev. Lett. **81**, 1682 (1998).
[11] M. Behet, S. Nemeth, J. De Boeck, G. Borghs, J. Tuemmler, J. Woitok, and J. Geurts, Semicond. Sci. Technol. **13**, 428 (1998).
[12] Handling Recommendations for e-beam Negative-Tone Resist AZ PN114, Hoechst Celanese Corporation, Route 202-206 North, P.O. Box 2500, Sommerville, NJ 08876, 1991.
[13] I. O. Kulik, Zh. Éksp. Teor. Fiz. **57**, 1745 (1969) [Sov. Phys. JETP **30**, 944 (1970)].
[14] G. F. Giuliani, and J. J. Quinn, Phys. Rev. B **26**, 4421 (1982).
[15] H. Pothier, S. Guéron, N. O. Birge, D. Esteve, and M. H. Devoret, Z. Phys. B **104**, 178 (1997).
[16] D. Uhlisch, Ber. Forschungszent. Jülich **Jül-3490**, 1 (1997).
[17] J. Gu, W. Cha, K. Gamo, and S. Namba, J. Appl. Phys. **50**, 6437 (1979).